Wind and earthquake effects on the nonlinear response of steel braced frame buildings

Anastasia Athanasiou[1], Lucia Tirca[2], Ted Stathopoulos[3]

[1] Post-doc fellow, Depart. of Building, Civil and Environmental Engineering, Concordia University - Montreal, QC, Canada.
[2] Associate Prof., Depart. of Building, Civil and Environmental Engineering, Concordia University - Montreal, QC, Canada.
[3] Professor, Department of Building, Civil and Environmental Engineering, Concordia University - Montreal, QC, Canada.

ABSTRACT

The response of multi-storey steel buildings to earthquake and wind loads is challenging. In general, the design of ductile steel buildings with an aspect ratio ≥ 2 could be controlled in one direction by wind and in the orthogonal direction by earthquake. Wind demands on buildings designed to earthquake loads tend to produce larger drift at upper floors exceeding the serviceability limit state and greater shear force at the lower half floors. Up to date, a few studies have focused on the nonlinear response of structures subjected to wind loads. The cause could be the complex nature of wind signals and the significant computational effort required to perform nonlinear time history response analysis under wind load. This paper assesses the dynamic performance of a mid-rise concentrically braced frame building designed to resist multi-hazard type of loadings: earthquake and wind. The prototype building of normal importance category is a 15-storey steel braced frame building with a 1:2 aspect ratio located on Site Class C in downtown Montreal. This building is designed according to the NBCC (2015) and CSA/S16 (2014) standard. Dynamic wind time histories on the windward and leeward directions are generated using wind tunnel pressure records available at the Tokyo Polytechnic University aerodynamic database. A sophisticated nonlinear model of the structure with distributed plasticity is developed in OpenSees. The model is used for the simulation of the dynamic behavior of the lateral load resisting system to earthquake and wind events of increasing return period. The main objectives of this study are: i) to generate a set of along-wind, wind load time series using wind tunnel tests data, ii) to perform nonlinear wind analyses of the building; iii) to compare the overall response of the dynamically sensitive building to strong motion and wind excitation; and iv) to calculate the residual drift under the provided wind time-history loading versus earthquake loading.

Keywords: wind engineering, earthquake effects, steel structure, nonlinear dynamic analysis

INTRODUCTION

Wind engineering has been developed rapidly since the 70s, however, the evaluation of the dynamic performance of tall structures under wind loads is challenging. In the last decade, researchers started to apply the earthquake engineering know-how to investigate the nonlinear behavior of buildings under wind loads. Van de Lindt et al. [1] proposed a performance-based-design wind engineering framework and used it for the wind assessment of wooden buildings. The authors used a detailed physical model of a wooden structure and developed fragility curves to describe four performance expectation levels: occupancy comfort, continued occupancy, life safety and structural instability. The occupancy comfort and structural instability states were firstly introduced by the authors. The performance descriptors were defined considering the performance of the roof, the building envelope and the lateral resisting system. The authors used the 3-second peak gust speed in 50 years to define the specific hazard level. The wind forces were calculated as per ASCE 7-05 [2] following the code-compliant static approach, i.e. neglecting the dynamic nature of wind and its effect on the building performance. A similar performance based approach was proposed by Griffis et al. [4] for the economic design of wind resistant structures. The authors defined seven wind hazard levels following ASCE 7-10 [3] and ATC [5]. The American Standards provide statistical, site-specific wind climate models which link the expected wind speeds to distinct mean recurrence intervals. The authors proposed the use of deformation descriptors (drifts, rotations) to account for light to zero damage in the overall system. Muthukumar et al [6] applied the framework proposed by Griffis et al [3] for the vulnerability assessment of an existing high-rise building. Recently, Santos-Santiago et al. [7] evaluated the dynamic response of a 28-story moment frame building in Mexico City to earthquake and wind loads. The authors performed nonlinear seismic and wind analyses and developed fragility curves at three distinct damage levels (minor, moderate, and severe). The earthquake- and wind-induced damage was quantified using the peak interstorey drift and the peak floor acceleration, respectively. Judd and Charney [8] investigated the inelastic behavior and probability of collapse of a 10-story building through nonlinear dynamic analyses of an equivalent SDOF model. A set of wind loads was developed using wind pressure records available in the Tokyo Polytechnic University database (http://www.wind.arch.t-kougei.ac.jp). The TPU database is commonly used in literature for the study of wind effects on buildings [9, 10, 11]. Recently,

Judd [11] developed a refined, nonlinear, finite element model of the 10-story building and subjected it to extreme wind hazards levels. This study overcomes the limitations of the previous one, arising mainly due to the simplicity of the considered model.

It is clear that the existing studies on the nonlinear wind performance of structures are limited and still exploratory in nature. The linear, pseudo-static wind design approach is well-established in the engineering practice and further research is required before the major international codes adopt more sophisticated, dynamic approaches, such as the ones implemented for the seismic design of structures. The National Building Code of Canada (NBC-2015, [12]) adopts a simple, pseudo-static approach for the definition of earthquake and wind- induced loads. However, the seismic base shear is further reduced by the factor R_dR_o, which accounts for the overstrength (R_o) and inherent ductility of structural members (R_d). The building is designed to yield under the earthquake design level, while should remain in the linear range under the factored nominal wind load. According to NBC-2015, the wind load factor equals to 1.4 and the provided wind pressure was calibrated for a tolerable annual failure probability of $3x10^{-5}$, or in other words, a target reliability index of 3 for a 50-year service life [13]. Thus, the factored design wind load corresponds to wind events with a return period of approximately 500 years, while the nominal wind load is specified using the 50-year return period value of the hourly mean wind speed [13]. If the nominal overstrength factor R_o=1.3 was considered, the structure would resist wind loads with return periods of 5,000-10,000 years. Meanwhile, the design earthquake load is associated to a return period of 2,400 years (2% probability of exceedance in 50 years). Hence, owing to the different distribution of return periods, there is a significant difference in the annual probabilities of occurrence of seismic and wind events. In fact, there are more days of noticeable wind than days of noticeable earthquake. The earthquake input forces for a 50-year return period are only 15% of those corresponding to a 2,500-return period, while the wind pressures based on a 50-year return period are about 60% of the corresponding pressures based on a 2,500-return period wind [13].

The present paper focuses on the dynamic response simulation of mid-rise steel office building structure under recurring earthquake and wind loads. The input wind forces are generated from wind tunnel data on a similar scaled structure, available at the Tokyo Polytechnic University Aerodynamic database, and are scaled linearly to provide increasing levels of the wind hazard. A sophisticated nonlinear model of the structure developed in OpenSees [14] is used to assess the system performance in terms of interstorey drift, residual interstorey drift and floor acceleration. The presented results are preliminary in nature and set the basis for further developments in multi-hazard performance assessment in the near future.

CASE STUDY

The case study is a 15-storey Concentrically Braced Frame (CBF) building constructed on dense soil (Site Class C) in downtown Montreal. The building height is 54.4 m, the typical storey height is 3.6 m and that of ground floor is 4.0 m. The bays are 7.5 m wide in both *X* and *Y* directions. The Lateral Force Resisting System (LFRS) displaced in each orthogonal direction consists of four moderately ductile (MD) concentrically braced frames with tension-compression multi-storey X-bracing configuration. The building is symmetric in plan and is regular in height as illustrated in Figure 1. The building occupancy type is office which is normal importance category [12]. The roof and typical floor dead load is 3.4 kPa and 4 kPa, respectively, the snow load is 2.48 kPa and the live load is 2.4 kPa for typical floor. Considering 1.5 kPa for cladding and 25% snow load at the roof level, the total seismic weight of the building is W = 169,670 kN. According to[12], the fundamental period of the building is estimated as $T_a = 0.05h_n$,where h_n is the total building height. For this case study, T_a is 2.72 s.

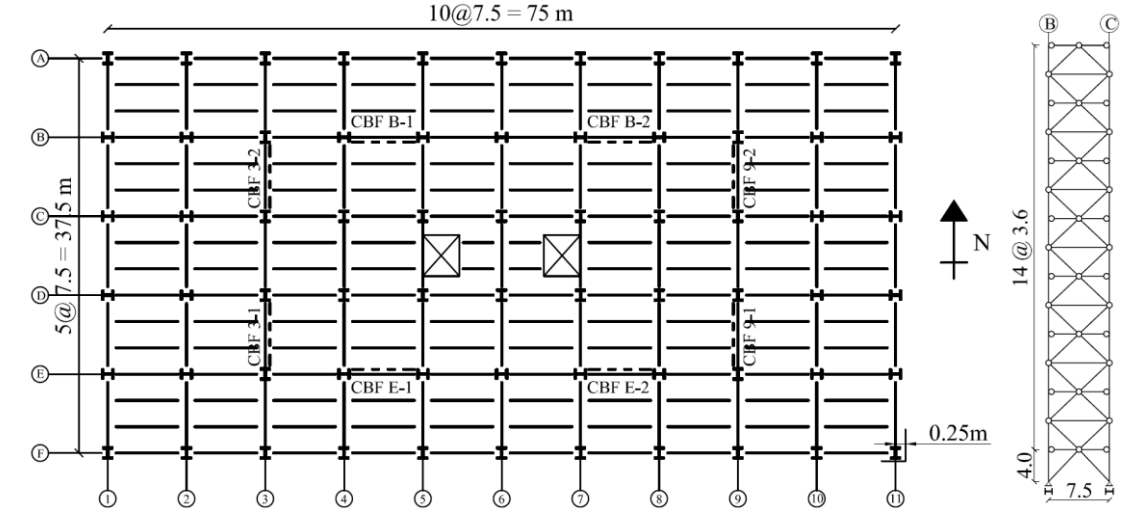

Figure 1: a) Typical floor plan, and b) N-S elevation associated with the numerical model of ¼ floor area.

To design the 15-storey CBF building to seismic load, firstly, the equivalent static force procedure defined in [12] is employed and the base shear used in design cannot be lower than $V_{min} = I_E S(2.0) M_v W / R_d R_0$, where I_E is the earthquake importance factor, S(2.0) is the design spectral response acceleration expressed as a ratio of gravitational acceleration for a period T= 2.0 s, M_v is the higher mode effect on base shear and R_d, R_0 are the ductility- and overstrength-related force modification factor, respectively. For this case study, $I_E = 1.0$, $M_v = 1.0$, S(2.0) = 0.068g and $R_d R_0 = 3.9$ which leads to $V_{min} = 2958$ kN. Using the inverted triangular distribution approach, the base shear was distributed along the building height and braces, beams, and columns are designed. Herein, torsion due to accidental eccentricity was neglected and P-delta effect was considered in the second iteration after the interstorey drift was computed. Beam and column members are made of W-shape and braces are made of square hollow structural sections, HSS. The steel yield strength is $F_y = 350$ MPa and the probable yield stress used in capacity design was taken as $R_y F_y$. According to CSA-S16-14 standard [15], $R_y = 1.1$ is associated to W-shape sections and the product $R_y F_y = 460$ MPa to HSS sections.

To analyze the dynamic distribution of base shear along the building height and the associated interstorey drift values, a three-dimensional linear model of the structure was developed in ETABS. In the model, the braces to frame connections and beams to column connections are simulated as pinned and the CBF columns are continuous over two stories [15]. The composite steel deck is assumed to behave as a rigid diaphragm and a 2% inherent damping was considered. The model was analyzed using the linear dynamic analysis by means of modal response spectrum method. From analysis, the first mode period in N-S direction is $T_1 = 3.41$ s and the resulted base shear is $V_{dyn} = 2395$ kN. Because the building is regular, V_{dyn} is slightly greater than $0.8V_{min}$ which is deemed acceptable according to [12]. The peak interstorey drift is within the code limit of 2.5% h_s where h_s is the storey height. When P-delta effect was considered a few braces required a slightly larger cross-section. The brace, beam, and column sections are provided in Table 1.

Table 1: CBF sections

story	Braces	Beams	Columns
15	HSS114.3x114.3x6.4	W530x182	W250x58
14	HSS114.3x114.3x6.4	W460x128	W250x101
13	HSS 127 x127 x8.0	W460x128	W250x101
12	HSS 127 x127 x8.0	W460x128	W250x167
11	HSS152.4x152.4x7.9	W460x128	W250x167
10	HSS152.4x152.4x7.9	W460x128	W310x313
9	HSS152.4x152.4x9.5	W460x128	W310x313
8	HSS152.4x152.4x9.5	W460x158	W310x375
7	HSS152.4x152.4x9.5	W460x158	W310x375
6	HSS152.4x152.4x9.5	W460x158	W310x454
5	HSS152.4x152.4x12.7	W460x158	W310x454
4	HSS152.4x152.4x12.7	W460x158	W360x551
3	HSS152.4x152.4x12.7	W460x158	W360x551
2	HSS152.4x152.4x12.7	W460x158	W360x677
1	HSS177.8x177.8x12.7	W460x158	W360x677

With a fundamental frequency as low as 0.29 Hz ($T_1 = 3.41$ s) the building is classified as dynamically sensitive under wind load [12]. Thus, to verify the CBF members' sections to wind load the dynamic procedure is required. According to dynamic procedure, the exposure factor C_e and gust factor C_g are calculated differently than in the case of the static procedure. The specified external pressure acting statically in the direction normal to the surface is calculated as follows: $p = I_w q C_e C_t C_p C_g$ where I_w is the wind importance factor, q is the reference velocity pressure 1/50 years, C_t is the topographic factor and C_p the external pressure coefficient. In this case study, the direction of wind loading is considered N-S (larger cladding surface) and the I_W, C_t, q and C_p parameters are: $I_w = 1$, $C_t = 1.0$, q = 0.42 kPa, $C_{p(windward)} = 0.8$ and $C_{p(leeward)} = -0.5$. To design the main structural system on rough terrain, according to the dynamic procedure, the exposure factor is calculated as: $C_e = 0.5(h/12.7)^{0.5}$. For the windward surface, C_e decreases from roof to lower floors but cannot be less than 0.5, while for the leeward surface, C_e is constant along the building height and is calculated for the reference height, which is half of the total building height. The gust factor C_g is calculated as follows: $C_g = 1 + g_p(\sigma/\mu)$ where g_p is the peak factor depending on the average fluctuation rate, ν and the ratio σ/μ depends on the background turbulence factor (B), gust energy ratio (F), damping ratio (e.g. $\beta = 0.02$ for steel structures) and size reduction factor, s. From calculation it resulted $C_g = 2.43$. The factored wind base shear, 1.4W = 5384 kN, is less than the elastic seismic base shear which means that earthquake load governs the design. However, under factored wind load, the response of structure should be elastic and the interstorey drift should be less than 1/400 of storey height which corresponds to $0.25\%h_s$.

Accounting for the building's symmetry, the seismic load applied in N-S direction was distributed equally to the four CBFs (ranging from 1 to 4) in Figure 1. The tension-compression braces were designed to sustain factored seismic forces such that the factored axial force, C_f is less than or equal to the member resistance, C_r computed according to [15]. The ratio C_f/C_r along the building height is plotted in Figure 2a. Since the design of braces was earthquake-based, the resistance factors C_f/C_r take values which are less than or equal to 1 under the earthquake load. The wind demand verification showed that the corresponding wind resistant factors C_f/C_r, evaluated using the factored wind loads (1.4W), take values that are greater than one in the stories where wind loads are prevalent (stories 3 and 7). However, it was anticipated that the excessive wind forces will be accommodated by the overstrength of the members, and hence the lower floor brace sections were not further increased. Figures 2b and 2c show the peak earthquake and wind demand in terms of cumulative storey shear and interstorey drifts. As depicted in Figure 2b, there is only a slightly larger wind demand when the dynamic procedure is applied for the 15-storey building with an aspect ratio of 2. Conversely, the wind-induced shear may govern the design of lower-storey members when the overstrength and inherent ductility of the structure are neglected. The interstorey drifts under the service wind 0.75W, where W is the nominal wind load, do not exceed the limit value of 1/400, commonly used in wind design practice. The earthquake-induced drifts take values as high as 0.8% and tend to be higher at the upper floors.

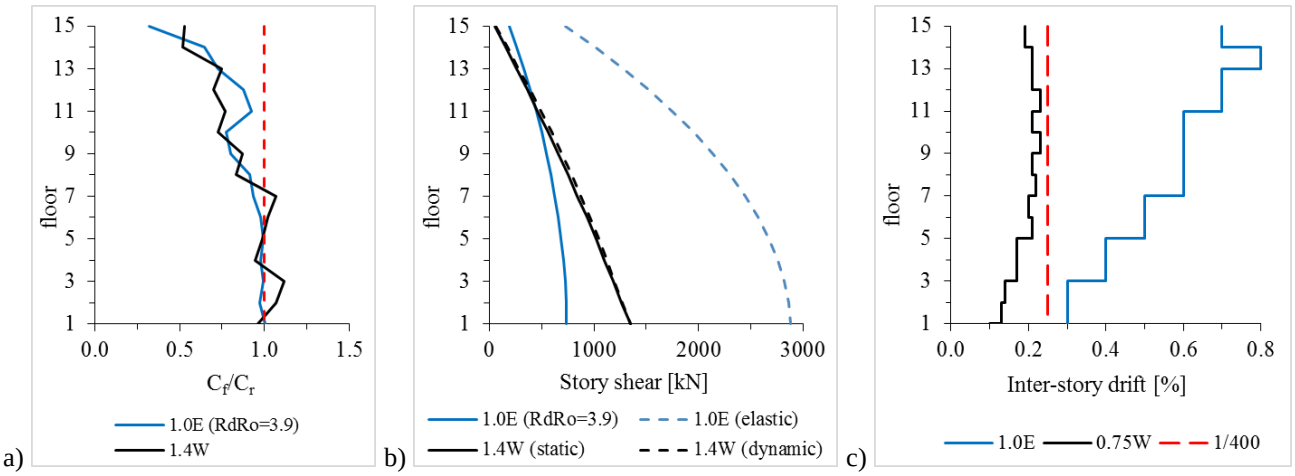

Figure 2: a) Resistance factors for the braces of the CBF 3-1, b) Cumulative story shear and c)Elastic interstorey drift demand under wind and earthquake design levels.

Modelling aspects

Due to the double symmetry of the building geometry with respect to *X* and *Y* axes, only one quarter of the structure is considered in design. Thus, only the 15-storey CBF 3-1 displaced in the N-S direction and the associated gravity columns were modelled in OpenSees (Figure 1b). The model accounts for the tensile yielding and buckling of HSS braces, the deformation and yielding of the gusset plate connections, but also the local yielding of beams and columns adjacent to braces. Force-based nonlinear beam–column elements with distributed plasticity and three integration points per element are used to model the HSS braces and the W-shape beams and columns of the CBF. Fiber discretization models are used to replicate steel sections with plane strain compatibility. The Giuffre–Menegotto–Pinto model is used to simulate the steel material assigned to braces, beams and columns. A calibrated fatigue material was assigned to HSS braces to capture the brace fracture caused by low-cycle fatigue. More information on the calibration of fatigue model may be found in [16]. Each brace is made of 16 nonlinear beam-column elements with distributed plasticity and an initial out-of-plane imperfection set to 1/500 of the effective brace length was assigned to allow buckling. The imperfection ratio for the CBF beams and columns is set to 1/1000. To capture large deformations, the co-rotational coordinate transformation is applied for non-linear members. The brace-to-frame gusset plate connection is simulated using two rotational springs and one torsional spring assigned in the zero-length element connecting the brace to a rigid link. The first-mode period of the system, before the first yielding, equals T_1=3.58 s, i.e. 5% higher than the value calculated using ETABS. The first mode is purely translational.

Earthquake hazard

Due to lack of historical ground motions in Easter Canada, a suite of artificial records corresponding to Site Class C in Montreal, developed by Atkinson is considered (www.seismotoolbox.ca). These artificial records correspond to earthquakes of magnitude 7 and the epicentral distance varies from 13.8 km to 50.3 km. According to NBC 2015, the minimum number of records used in analysis should be not less than 11. However, for a defined scenario-specific target spectrum, using fewer than 11 records per suite is permitted but the number should not be less than 5. In this study, 7 records are considered and their seismic

characteristics are provided in Table 2. Herein, the PGA and PGV are the peak ground acceleration and peak ground velocity, respectively, t_D is the Trifunac duration, T_p is the main period of ground motion record and T_m is the mean period. These records are scaled according to [12] such that the mean spectrum of a suite of minimum records discussed above is not less than 90% of the design spectrum in the period range of $0.2T_1$ to $1.5T_1$. The design spectrum for Montreal associated to 2%, probability of exceedance in 50 years, the scaled spectrum of each record and their mean response spectrum are depicted in Figure 3. The duration of each selected ground motion is approximately 20 s. However, to capture the response of the model to free vibrations, another 20 s of zero amplitude were added to each record.

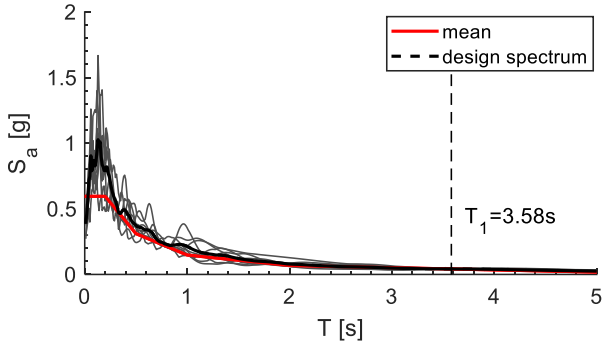

Figure 3: Elastic response spectra of selected records, the design spectrum and the mean spectrum.

Table 2: Ground motions characteristics and scaling factors.

Event	M_w	Station	PGA [g]	PGV [m/s]	PGV/PGA	t_D [s]	T_p [s]	T_m [s]	Scale factor
M7C1-13.8	7.0	Simulated	0.727	0.370	0.052	7.180	0.120	0.244	0.60
M7C1-20.1	7.0	Simulated	0.653	0.396	0.062	6.012	0.140	0.296	0.70
M7C1-25.2	7.0	Simulated	0.386	0.187	0.049	7.320	0.060	0.243	1.10
M7C1-25.6	7.0	Simulated	0.339	0.194	0.058	7.846	0.160	0.266	1.20
M7C1-25.8	7.0	Simulated	0.293	0.178	0.062	7.308	0.080	0.282	0.90
M7C2-41.6	7.0	Simulated	0.229	0.144	0.064	7.614	0.140	0.306	1.30
M7C2-50.3	7.0	Simulated	0.151	0.075	0.051	8.744	0.160	0.277	2.50

Wind hazard

No full scale wind response records seem to be available in the literature. Regardless, their use would be limited; wind records are case-specific owing to the complex aerodynamic interaction of the flow with the building environment. Herein, a set of windward and leeward force histories were applied to each story level. The forces are generated using a set of normalized, wind tunnel pressure histories available at the Tokyo Polytechnic Aerodynamic Database (http://www.wind.arch.t-kougei.ac.jp/system/eng/contents/code/tpu). The tested prototype was a 1:400-scaled model of a high-rise structure characterized by height-breadth-depth ratios similar to those of the building considered herein. Figure 4 shows the fluctuating pressure spectra of two signals obtained from the pressure taps located in the mid-height of the windward and leeward cladding surface. The moving averaged, smoothed spectra are also shown in red color. The forces were evaluated by multiplying the normalized pressure coefficients by the reference wind pressure at roof height, p_H and the corresponding tributary area. The evaluated pressure p_H makes reference to the NBC design wind level (one in a 50-year wind speed, V_{10}=25.5m/s). As a consequence, the calculated wind histories are of the same order of the nominal wind loads, evaluated as per the dynamic procedure given in NBC-2015. While both earthquake and wind histories are random signals, they are characterized by different

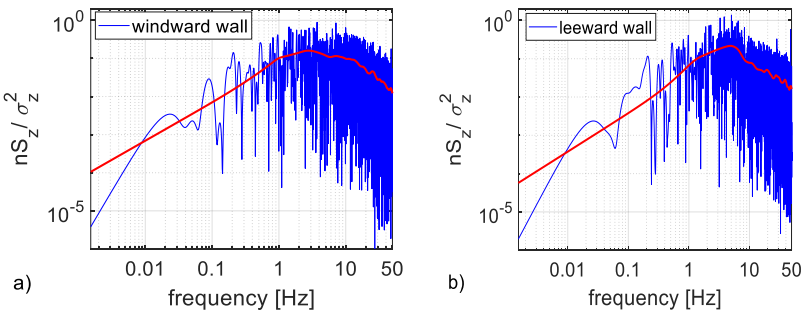

Figure 4: Spectra of the fluctuating pressure acting at the mid-height of a) windward and b) leeward walls.

duration and frequency content. The full scale of the wind records considered is 72 min, i.e. 240 times longer than the motions used in the earthquake response analyses. Moreover, the wind signals are characterized by a broader frequency content. Figure 5 shows a comparison between typical Fourier amplitude spectra for the wind and earthquake records considered. For convenience, both spectra are normalized by their peak values. While the wind Fourier spectrum covers a broad frequency range from 0.01 to 10 Hz, the earthquake spectrum is clearly more evident for frequencies above 0.1 Hz, i.e. the range of frequencies most hazardous for building structures.

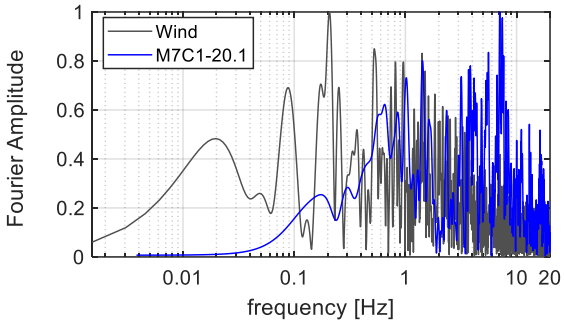

Figure 5: Normalized Fourier Amplitude spectra of two considered windward and simulated earthquake records.

Building response to nonlinear numerical analyses

This section summarizes the output of eleven nonlinear response history analyses performed in OpenSees [14]. Firstly, the model is subjected to seven scaled ground motions given in Table 2. Secondly, the model is subjected to four levels of generated wind loading histories. The coefficient applied to wind loading is increased from 0.75 (service wind, V_{10} = 22.1 m/s^2), to 1.0 (nominal wind, V_{10} = 25.5m/s^2), 1.4 (factored wind load, V_{10} = 30.2m/s^2) and 1.55 (increased factored wind load, V_{10} = 32.3m/s^2). The first wind hazard level refers to the serviceability limit state and the following two levels to ultimate limit states. Figures 6 and 7 show the distribution of seismic and wind response along the building height expressed in terms of interstorey drifts (a), residual interstorey drifts (b) and floor accelerations (c). The model responds nonlinearly to the input seismic motions. Furthermore, the peak of mean interstorey drift among floors is 1.4% h_s and occurs at top floors, the peak of mean residual interstorey drift is 0.2% h_s and the peak of mean floor acceleration is 0.55g. As depicted, the drift-induced damage is concentrated at upper floors, while floor acceleration shows a uniform distribution. When the system is subjected to time-history wind loading, it remains in the linear range under the service, nominal, and factored wind load (0.75W, 1.0W and 1.4W). However, under the service wind load (0.75W), the upper half floors exhibit interstorey drifts slightly larger than 1/400 storey height. It is noted that a small increase of loading factor from 1.4 to 1.55 leads to excitations of the system in the nonlinear range. To summarize, the earthquake demand is mostly concentrated at the upper three floors, while the wind demand imposes greater shear force at the lower half floors and larger drifts at the upper half floors. Figure 2a shows that braces of stories 3 and 7 were under-design to wind force by about 10%. These stories undergo drift concentration when the CBF braces respond in

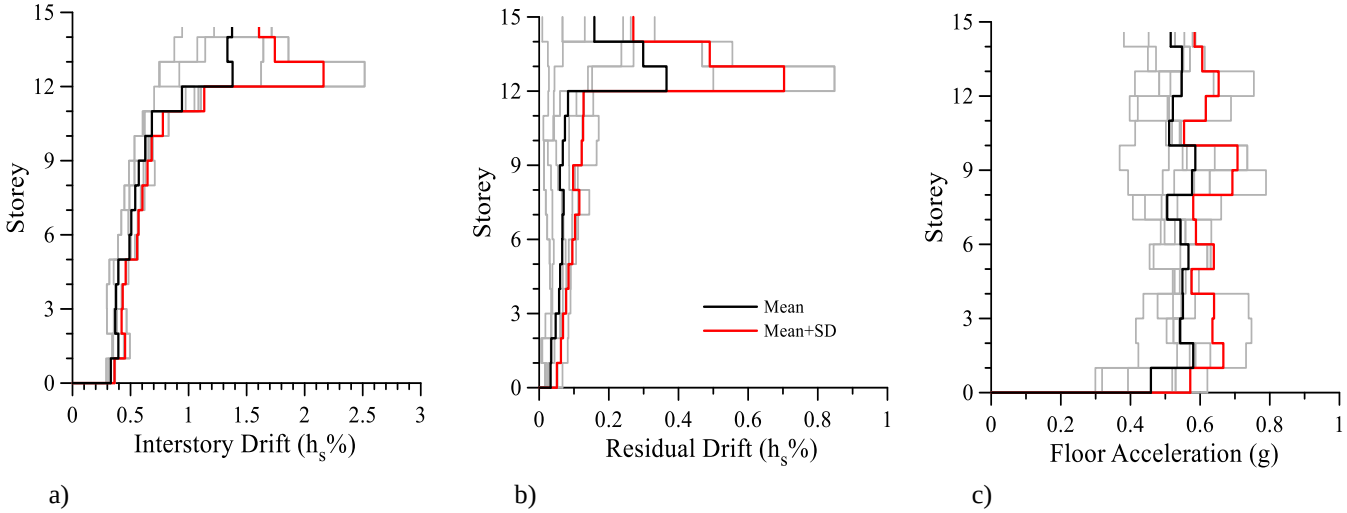

Figure 6: Building response to NBC-spectrum compatible ground motions in terms of: a) interstorey drifts, b) residual interstorey drifts, and c) relative floor accelerations.

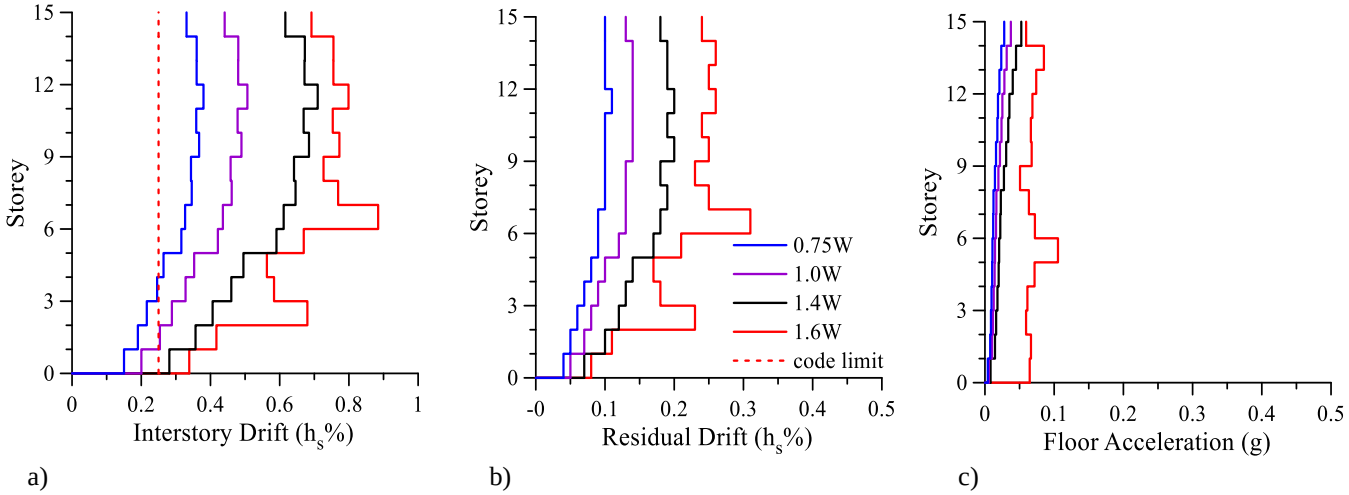

Figure 7: Building response to four levels of wind excitation (0.75W, 1.0W, 1.4W, 1.6W) in terms of: a) interstorey drifts, b) residual interstorey drifts and c) relative floor accelerations.

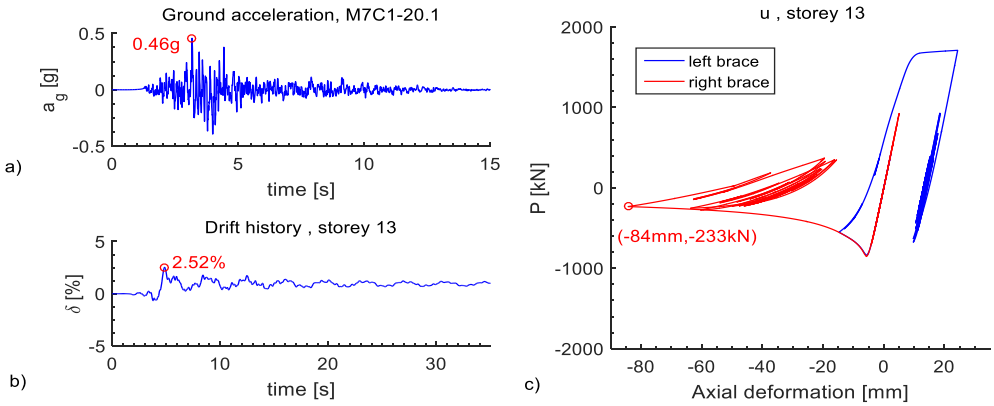

Figure 8: a) Input ground motion, b) time-history interstorey drift at 13th floor and c) force-displacement response of the left and right HSS braces of the 13th story under the M7C1-20.1 motion.

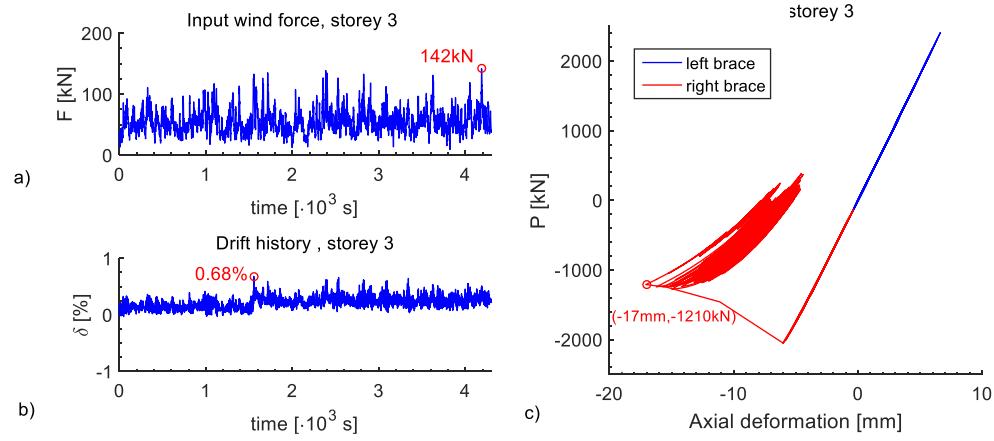

Figure 9: a) Input wind force, b) time-history interstorey drift at 3rd floor and c) force-displacement response of the left and right HSS braces at 3rd floor under the highest factored wind load, 1.55W.

nonlinear range under 1.55W which is greater than the design level (1.4W). Figure 8 shows the nonlinear response of the 13th floor to the M7C1-20.1 record scaled to code design spectrum. Similarly, Figure 9, illustrates the nonlinear response of the 3rd floor under wind load scaled 10% above the ultimate limit state (1.4W). The accelerogram plotted in Figure 8a has an almost symmetric shape and the peak of 0.46g is reached at t = 3.7 s. The time-history series of floor interstorey drift plotted in Figure 8b shows a peak of 2.52% h_s which is about the upper code limit. The hysteresis response of tension and compression HSS

braces located at the same floor shows yielding in tension and buckling in compression (Figure 8c). As depicted in Figure 9a, the wind loading is skewed; the input wind forces take only positive values and as a result the system under wind load vibrates about an equilibrium position that is different than zero. While the wind-induced drifts at the service, nominal, and factored wind levels are almost half the seismic induced drifts, they take values that are higher than the accepted code based limit of 1/400. The drifts at the service wind load are 30-50% higher than the code limit (stories 7 to 15), and take their maximum value at the 12th floor. For the drifts to be reduced and satisfy the code-prescribed limit, the members' stiffness should be increased accordingly. Due to the long duration of the wind load (72 min, approximately one hour) the braces are subjected to dozens of cycles with diminishing energy dissipation capacity, as depicted in Figure 9c.

CONCLUSIONS

The presented paper focuses on the dynamic response simulation of a 15-storey steel office building under earthquake and wind loads. The input wind forces are generated from wind tunnel data on a similar scaled structure, available at the Tokyo Polytechnic University Aerodynamic database, and are scaled linearly to provide increasing levels of the wind hazard. A sophisticated nonlinear model of the structure with distributed plasticity is developed in OpenSees and used to assess the system performance in terms of interstorey drift, residual interstorey drift and floor acceleration. The results show that the current, elastic design of wind-excited structures is conservative and could further benefit from the consideration of the overstrength and the inherent nonlinearity of the structure. Conversely to the design earthquake loads, that have a reference return period of 2,400 years, the service and design level wind events occur in short period intervals (1 in 50-year). However, a small increase in the wind load factor leads to a significant change in the wind return period. Hence, the consideration of the system nonlinearity is essential for the economic design of structures excited at different hazard levels. The presented results are preliminary in nature and set the basis for further developments in multi-hazard performance assessment in the near future.

ACKNOWLEDGMENTS

The authors would like to acknowledge the financial support of the Québec Fonds pour la Recherche sur la Nature et les Technologies (FQRNT) for the Centre d'Études Interuniversitaires des Structures sous Charges Extrêmes (CEISCE).

REFERENCES

[1] Van de Lindt, J. W., and Dao, T. N. (2009). "Performance-based wind engineering for wood-frame buildings." *Journal of Structural Engineering*, 135(2), 169–177.

[2,3] American Society of Civil Engineers, ASCE (2005) and (2010) "Minimum design loads for buildings and other structures." Reston, Va.

[4] Griffis, L., Patel, V., Muthukumar, S., and Baldava, S. (2012). "A framework for performance-based wind engineering." In Advances in Hurricane Engineering, 1205-1216.

[5] ATC (Applied Technology Council) (2018). "Wind speed by location". Accessed February 13, 2012. http://windspeed.atcouncil.org/

[6] Muthukumar, S., Baldava, S., and Garber, J. (2012). "Performance-based evaluation of an existing building subjected to wind forces." In Advances in Hurricane Engineering, 1217–1228.

[7] Santos-Santiago M. A., Ruiz S. E., and Valenzuela-Beltrán F. (2018). "Multi-hazard risk assessment (seismic and wind) for buildings with dampers in Mexico City". In 11th U.S. National Conf. on Earthquake Eng., Los Angeles, California.

[8] Tamura, Y., Suganuma, S., Kikuchi, H., and Hibi, K. (1999). "Proper orthogonal decomposition of random wind pressure field." Journal of Fluids and Structures, 13, 1069–95.

[9] Huang, G., and Chen, X. (2007). "Wind load effects and equivalent static wind loads of tall buildings based on synchronous pressure measurements." Engineering Structures, 29, 2641-2653.

[10] Judd, J. P., and Charney, F.A. (2015). "Inelastic building behavior and collapse risk for wind loads." In Structures Congress 2015. Reston, VA: ASCE.

[11] Judd, J.P. (2018). "Windstorm Resilience of a 10-Story Steel Frame Office Building". Journal of Risk and Uncertainty in Engineering Systems, Part A: Civil Engineering, 4(3): 04018020-10.

[12] NRCC, National Building Code of Canada (2015), 14th ed. National Research Council of Canada, Ottawa, ON, 2015.

[13] Structural Commentary part I (2017) "Wind load and effects, User's Guide - NBC 2015: Part 4 of Division B", National Research Council of Canada, Ottawa.

[14] PEER (Pacific Earthquake Engineering Research Center). (2015). Open systems for earthquake engineering simulation (OpenSees)

[15] CSA, CSA S16–14, Canadian Standards Association (CSA) (2014). "Design of Steel Structures". S16.-14 Standard, CSA, Mississauga, ON.

[16] Bosco M., and Tirca L. (2017). "Numerical simulation of steel I-shaped beam using a fiber based damage accumulation model". Journal of Constructional Steel Research, Volume 13.